Available online at www.sciencedirect.com

SciVerse ScienceDirect

Procedia Engineering 49 (2012) 324 – 329

Procedia Engineering

www.elsevier.com/locate/procedia

Evolving Energy-IEF International Energy Congress (IEF-IEC2012)

Experimental analysis of two-phase flow nozzle for desalination and power generation system

Sara Vahaji*, Abhijit Date, Sherman C. Cheung, Jiyuan Tu, Aliakbar Akbarzadeh, M.Oreijah

School of Aerospace, Mechanical and Manufacturing Engineering, P.O. Box: 71, RMIT University, Bundoora, 3083, Australia

Elsevier use only: Revised 30th August 2012; accepted 31st August 2012

Abstract

This paper presents theoretical and experimental performance analysis for two-phase flow nozzle. Governing equations have been discussed with the performance predictions for different inlet temperatures and outlet pressures. Different size nozzles have been tested for varying inlet and outlet conditions. The experimental results have shown that for simple nozzle geometry (orifice) the expansion is far away from a complete isentropic expansion. Reaction force measurements for an ideal condition (i.e. isentropic expansion) and real condition are compared and discussed.

Keywords: two phase nozzles; thermal desalination; power generation; renewable energy; flashing.

Nomenclature

F	force (N)
h	enthalpy (m^2/s^2)
L	length of nozzle (mm)
m	mass flow rate (kg/s)
P	pressure (kPa)
T	temperature (°C)
x	quality
Greek symbols	
α	void fraction
ϑ	specific volume (m3/kg)
v	velocity (m/s)
ε	efficiency factor
Subscripts	
e	property at nozzle exit
G	gas
in	property at nozzle inlet
L	liquid
sat	saturation

* Corresponding author. Tel.: +61-3-99256187.
E-mail address: sara.vahaji@rmit.edu.au

 doi:10.1016/j.proeng.2012.10.144

1. Introduction

Exponential increase in world population and reduced rain in certain areas of the world has led to a fresh water shortage. In addition to this the technological advances and industrialization has led to increase demands for power and our dependency on fossil fuels.

Figure 1 demonstrates the global distribution of the world's water (UN GEO-4 2007). Considering the population growth and rapid pace of industrialization in developing countries, water shortage is a serious threat not only to the viability of the industry but also to the basic supply of drinking water. According to the report by the WHO (World Health Organization) and the UN, an estimated 2.6 billion people are living without improved sanitation facilities because of overexploitation and pollution of water. If the 1990-2002 trends continue, the world will miss the sanitation target of the MDG (Millennium Development Goals) by more than half a billion people (WHO and UNICEF 2004).

To solve the lack of water, many technologies have been developed over the past years to separate water and salt from saline water sources. Most commonly used method is heating saline liquid water to temperatures above 100°C to produce large amounts of vapour under atmospheric conditions and condense the vapour to get fresh water. In this method saline water is generally heated by burning fossil fuels. Burning fossil fuels results in generating greenhouse gases, which cause another threat to the environment. The second most common method of desalination of saline water is using reverse osmosis, where saline water is pressurized to respective osmotic pressures and passed through filters to separate salt and fresh water. For seawater with an average salinity of 2.5% the osmotic pressure is 2.6MPa which means that pump should overcome this pressure to make the fluid flow in the reverse direction [1].

The thermal desalination process uses the phenomenon of flashing or sudden boiling due to sudden or gradual depressurization of hot saline water. The process of flashing has been studied and investigated in past by many researchers and a good understanding of the flashing process has been developed [2-7]. Past studies have shown importance of super heat and the local pressure in the process of flashing. It is shown that rate of flash evaporation rises by increasing the initial water temperature and the superheat degree [8].

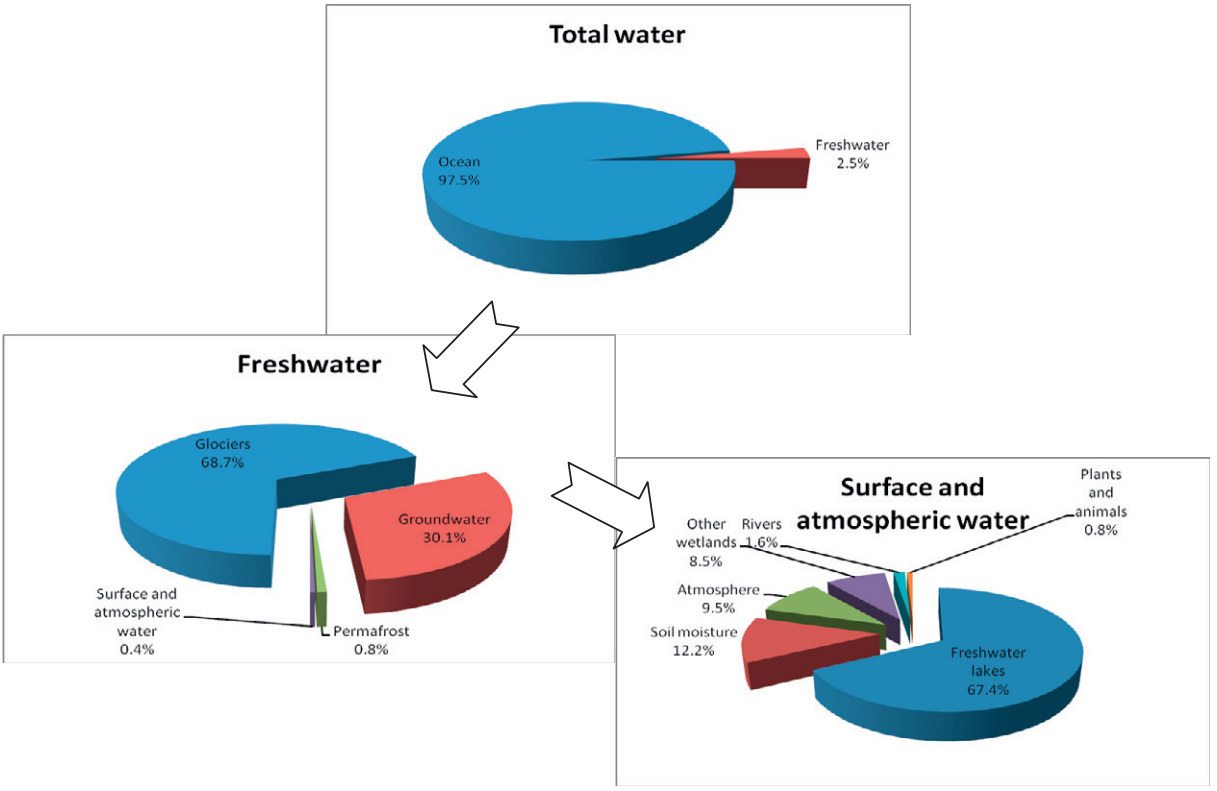

Figure 1. Global distribution of the world's water (recreated from UN GEO-4 2007).

In this method - Combined Desalination and Power generation (CDP) - saline water is heated up to 100°C at atmospheric pressure. Then it is introduced into an evacuated chamber through a simple orifice shape nozzle. As a result of experiencing the pressure difference between outside and inside of the chamber, saline water forms a mixture of liquid droplets and vapour. Later, vapour is condensed on the surface of the condenser and collected in the fresh water tank. Simultaneously, the reaction force caused by high velocity of mixture entering into the vacuum chamber, could be utilized to produce power.

Following are the advantages of the CDP over the commonly used distillation or desalination methods:

- Fresh water and power are produced simultaneously.
- Water would be heated only up to 100°C, which could be maintained through other methods rather than burning fossil fuels. This method eliminates the need to burn fossil fuels and hence avoids the generation of greenhouse gases.
- It is observed that intensity of flash evaporation is faster in superheated water jets comparing water pools and also water flowing in channels.

This paper presents the experimental performance results of hot water (88°C to 96°C) flashing under vacuum (5kPa - 10kPa absolute). Flashing nozzles are often used in thermal desalination systems and in past they have been investigated to achieve maximum flashing to produce more vapour and inturn fresh water. However, optimum nozzle geometry is not achieved yet. If the nozzle geometry is optimized, flashing will take place inside the nozzle resulting in more mixture velocity and in sequence, more thrust. This paper further investigated the two phase flashing nozzle to estimate the optimized geometry. An interesting application of this investigation is discussed in the paper. Reaction force produced due to the high exit velocity of the flashing (expanding) fluid is measured for different water inlet temperatures and vacuum pressures. Simultaneously mass flow rate of hot water intake is estimated from volume flow measurements. Applying the conservation of mass and momentum and knowing the nozzle geometry the exit velocities are estimated for the nozzle exits. Tests are repeated for different exit nozzle lengths to find out the best nozzle length.

2. Experimental set up

Figure 2 shows a simplified schematic of the test rig. Water is heated in the tank to boiling temperature at atmospheric pressure and introduced into the flashing tank where a vacuum of 5kPa (absolute) is maintained. This is achieved by connecting a vacuum pump to the flashing tank. Before water enters the inlet pipe any solid impurities are filtered to prevent clogging of the nozzle.

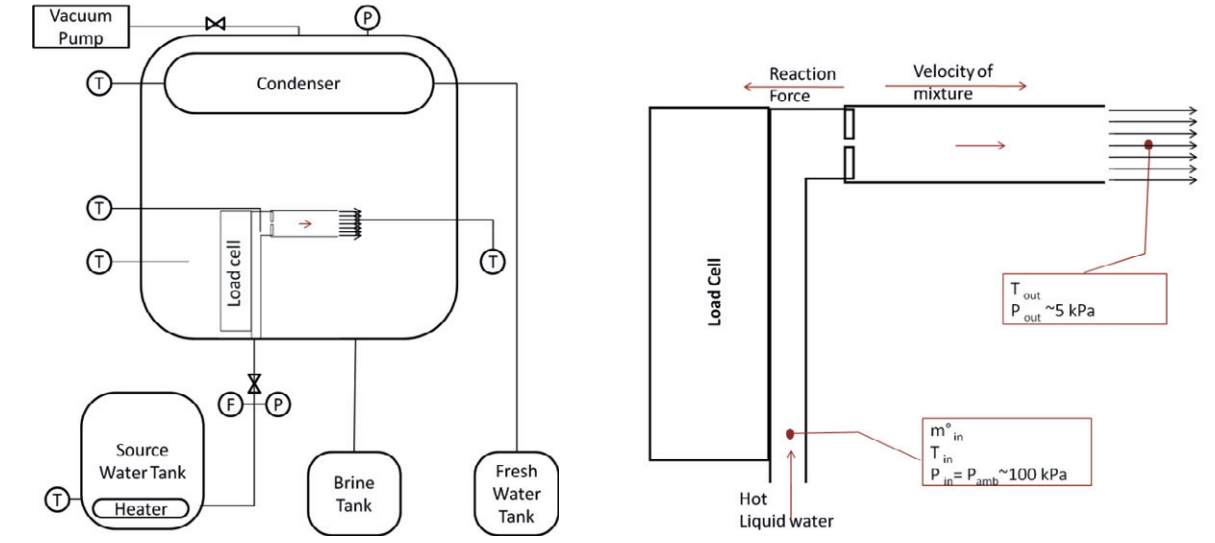

Figure 2. Schematic diagram for (a) the test rig and (b) the nozzle set-up.

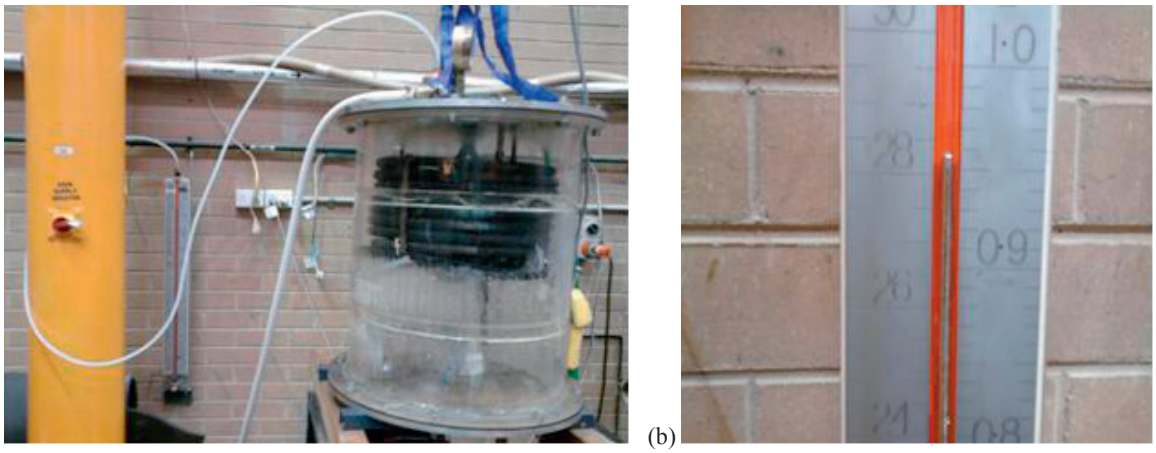

Figure 3. A mercury manometer used for measuring the pressure of the flashing tank (a) whole set up and (b) better view of the manometer reading.

The hot water moves rapidly from the atmospheric pressure region to a very low pressure region causing it to flash evaporate. It is expected that a homogenous mixture of the liquid and vapour would flow out of the nozzle at very high velocities and as a direct effect of this the nozzle will experience a big reaction force ($\dot{m} \times v$). Now the liquid portion of the mixture will eventually fall to the bottom plate and is collected in the brine tank, whereas the vapour would rise in the chamber. It is then condensed on the surface of the condenser and gets collected in the freshwater tank.

Temperature is measured at different positions like: at the inlet to the nozzle, at the exit of the nozzle, condenser inlet and outlet, and middle of the flashing tank. T-type thermocouples are used in the experimental set-up with an accuracy of $\pm 0.5^{o}C$.

The vacuum pressure inside the flashing tank is measured with a mercury manometer with a least count of 0.01 bar. This mercury manometer is shown in Figure 3. The ambient pressure (P_{amb}) is measured by a mercury barometer installed in the laboratory with a least count of ±0.01mmHg.

The reaction force created by the mixture fluid exiting from the nozzle is measured with a load cell. This load cell is mounted at the back of the nozzle and has an error less than 0.0067% relative output. The value of the force is logged through a digital Vishay strain indicator and recorder which is shown in Figure 4. To ensure the reliability of the readings, the strain indicator is calibrated at the beginning of each run by different weighs varying between the ranges of 7 to 400 grams. Then the correlation between force (m×g) and the readings from the strain indicator is determined. Now, the data given by strain indicator could be related to the value of the reaction force.

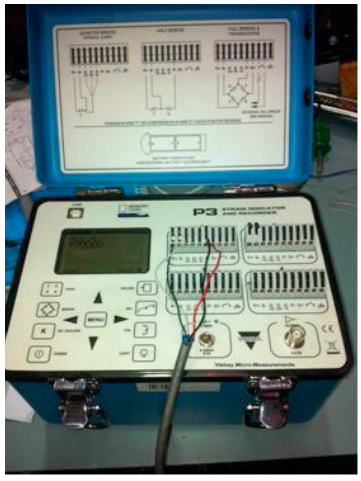

Figure 4. Vishay strain indicator and recorder.

3. Theoretical analysis

It is the main focus of this experimental study to achieve maximum reaction force. The ideal condition in theory is isentropic condition which is hardly achievable in real world. Hence, the isentropic case has been chosen as a reference for comparison of the experimental results.

Reaction force is measured by the load cell. In addition, the mass flow rate of the water (m_{exp}) entering into the system, inlet temperature and exit pressure are also measured. By substituting these values in the equations (1-4), quality, void fraction, velocity of the gas and velocity of the liquid at exit can be achieved.

$$m_{\exp} = \frac{v_{L,e}}{\vartheta_{L,e}} \frac{1-\alpha_e}{1-x_e} = \frac{v_{G,e}}{\vartheta_{G,e}} \frac{\alpha_e}{x_e} \tag{1}$$

$$F_{\exp} = \dot{m}_{\exp}\left[(1-x_e)v_{L,e} + x_e v_{G,e}\right] \tag{2}$$

$$h_{in} - h_e = (1-x_e)\frac{v_{L,e}^2}{2} + x_e \frac{v_{G,e}^2}{2} \tag{3}$$

$$h_e = (1-x_e)h_{L,sat}(P_{ex}) + x_e h_{G,sat}(P_{ex}) \tag{4}$$

Here we will define a new factor to express the efficiency of a real nozzle with respect to an isentropic nozzle. We call this factor as “Efficiency factor (ε)” which can be calculated as shown by equation (5).

$$\varepsilon = \frac{F_{\exp}}{\dot{m}_{\exp}\, v_{isentropic}} \times 100 \tag{5}$$

4. Experimental analysis

In figure 5. (a), (b) and (c), the degree of super heat (temperate difference between inlet, Th, and outlet of the nozzle, Tc) vs. measured force, the quality of the mixture and isentropic efficiency factor for three different nozzle lengths are shown. As a result, by increasing the superheat degree, higher force, quality and isentropic efficiency are achieved.

Figure 6. (a) and (b) show the experimental result for isentropic efficiency factor (ε) and force respectively in different lengths. Experiments show that in nozzle length equal to 160 mm, better isentropic efficiency and force is achieved rather than L=50 mm or L=210 mm. However, the highest isentropic efficiency factor achieved is only 13%. We believe that higher efficiency could be achieved by altering the geometry of the nozzle. It can be seen from the figure 6 that with the same exit diameter (12 mm) and same throat diameter (1.5 mm), the best nozzle length in terms of producing maximum reaction force is 160 mm. Further experimental investigation of different nozzle configurations needs to be carried out to improve the efficiency factor of the nozzle.

(a)**Error! Objects cannot be created from editing field codes.**

(b)**Error! Objects cannot be created from editing field codes.**

(c)**Error! Objects cannot be created from editing field codes.**

Figure 5. Experimental results for (a) superheat degree vs. force in three different nozzle lengths (b) superheat degree vs. mixture quality in three different nozzle lengths and (c) superheat degree vs. isentropic efficiency factor in three different nozzle lengths.

(a)**Error! Objects cannot be created from editing field codes.**(b)**Error! Objects cannot be created from editing field codes.**

Figure 6. Experimental results for (a) isentropic efficiency factor in different lengths and (b) force measured in different lengths.

5. Conclusion and future work

Based on the experimental result analysis, best nozzle length for the current nozzle configuration of 12mm exit diameter and 1.5mm inlet diameter is 160mm. However, nozzle configuration is not optimized yet and results can be improved. Nozzles that are used in experiments are orifice nozzles. Orifice is used because it has simple geometry which can be easily manufactured. However, in future convergent-divergent nozzles will be used in experiments and results will be compared. Another reason could be that mixture experiences higher back pressure inside the nozzle which leads in less evaporation rate and less reaction force. In future the author will continue the experiments to investigate the effect of other parameters i.e. larger exit area on the reaction force and achieve an optimized geometry of the nozzle which could result in better evaporation inside the nozzle and hence better reaction force.

Acknowledgements

We acknowledge that this project is supported by ARC Linkage under project ID. LP0990691. We also appreciate the financial support of Greenearth Energy Ltd, Australia.

References

[1] Thomso, A.M., 2003. Reverse-Osmosis Desalination of Seawater Powered by Photovoltaics Without Batteries.
[2] Brown, R., York, J.L., 1962. Sprays formed by flashing liquid jets. AIChE Journal **8**(2), p. 149.
[3] Gopalakrishna, S., Purushothaman, V. M.Lior, N., 1987. An experimental study of flash evaporation from liquid pools, Desalination 65, p.139.
[4] Peterson, R. J., Grewal, S. S.El-Wakil, M. M., 1984. Investigations of liquid flashing and evaporation due to sudden depressurization, International Journal of Heat and Mass Transfer 27, p.301.
[5] Kitamura, Y., Morimitsu, H.Takahashi, T., 1986. Critical superheat for flashing of superheated liquid jets, Industrial & Engineering Chemistry Fundamentals 25, p.206.
[6] El-Fiqi, A. K., Ali, N. H., El-Dessouky, H. T., Fath, H. S.El-Hefni, M. A., 2007. Flash evaporation in a superheated water liquid jet, Desalination 206, p.311.
[7] Mutair, S., Ikegami, Y., 2009. Experimental study on flash evaporation from superheated water jets: Influencing factors and formulation of correlation, International Journal of Heat and Mass Transfer 52, p.5643.
[8] Mutair, S., Ikegmi, Y., 2010. Experimental investigation on the characteristics of flash evaporation from superheated water jets for desalination, Desalination 251, p.103.
[9] Miyatake, O., Tomimura, T., Ide, Y., Yuda, M., Fujii, T., 1981. Effect of liquid temperature on spray flash evaporation, Desalination 37, p.351.